# Carrier capture processes in strain-induced $In_xGa_{1-x}As/GaAs$ quantum dot structures

C. Lingk, W. Helfer,* G. von Plessen, and J. Feldmann
*Photonics and Optoelectronics Group, Physics Department and CeNS, Ludwig-Maximilians-Universität, Amalienstraße 54, D-80799 München, Germany*

K. Stock†
*Walter Schottky Institut, Technische Universität München, Am Coulombwall, D-85748 Garching, Germany*

M. W. Feise and D. S. Citrin
*Department of Physics and Materials Research Center, Washington State University, Pullman, Washington 99164-2814*

H. Lipsanen and M. Sopanen
*Optoelectronics Laboratory, Helsinki University of Technology, Otakaari 1M, FIN-02150 Espoo, Finland*

R. Virkkala and J. Tulkki
*Laboratory of Computational Engineering, Helsinki University of Technology, FIN-02015 HUT, Finland*

J. Ahopelto
*VTT Electronics, Tekniikantie 17, P.O. Box 1101 FIN-02044 VTT, Finland*
(Received 26 May 2000; revised manuscript received 24 August 2000)

We investigate carrier capture processes in strain-induced quantum dot structures. The quantum dots consist of a near-surface InGaAs/GaAs quantum well in which a lateral confining potential is generated by the strain from InP stressor islands grown on the sample surface. Using photoluminescence spectroscopy, we show that the rate of carrier capture into the quantum dots increases dramatically when the energetic depth of the confinement potential is reduced by enlarging the quantum well/surface separation *D*. While carriers in the quantum well region between the quantum dots are found to experience *D*-dependent nonradiative surface recombination, this process seems to be negligible for carriers in the quantum dots, presumably due to the protecting InP islands.

## I. INTRODUCTION

Semiconductor quantum dots (QD's) confine electrons and holes in all three dimensions on a nanometer scale. Their special properties, such as the discrete density of states and low state degeneracy, are of interest for new optoelectronic devices such as QD lasers[1–3] and charge-storage devices.[4,5] In such devices, carriers are usually injected via some higher-dimensional barrier states and subsequently captured into the QD's, where they may undergo further energy relaxation between the QD levels. Both capture and relaxation may be slowed down due to the discreteness of the QD level structure, which hinders phonon emission.[6,7] This slowing down has been predicted to limit the speed of QD devices.[8] An additional problem connected to slow capture and relaxation may arise when parasitic processes, like nonradiative recombination at defects, compete with radiative or switching processes, and reduce the efficiency of devices.

In this work, we investigate carrier capture processes in strain-induced QD's. Such QD's are formed when strain exerted by stressor islands generates a lateral confinement potential in a nearby quantum well (QW). This class of QD's is of particular value for fundamental investigations due to their precisely known state degeneracies and optical selection rules, their equidistant and tunable energy-level splittings, and their high optical quality. They have been studied in investigations of carrier relaxation, magnetic-field effects, and strain effects,[9–17] and have been proposed for charge-storage devices.[18] The QD's investigated here consist of a near-surface InGaAs/GaAs QW in which a lateral confinement potential is generated by the strain from InP stressor islands grown on the sample surface. Using photoluminescence spectroscopy, we show that the rate of carrier capture into the QD's increases dramatically when the energetic depth of the confinement potential is reduced by enlarging the QW/surface separation *D*. While carriers in the QW region between the QD's are found to experience *D*-dependent nonradiative surface recombination, this process seems to be negligible for carriers confined in the QD's, presumably due to the protecting InP islands.

## II. SAMPLE GROWTH AND EXPERIMENT

The samples in this study were grown by metalorganic vapor phase epitaxy. The strain-induced QD's were fabricated by growing self-assembled InP islands on top of a buried 8-nm-thick $In_{0.2}Ga_{0.8}As$ QW as sketched in the upper part of Fig. 1. The InP islands were grown at a substrate temperature of 650 °C and have typical dimensions of 85 nm in width and 22 nm in height with an areal density of $1 \times 10^9\,cm^{-2}$ as determined by atomic force microscopy. These islands act as stressors on the underlying QW to form

 

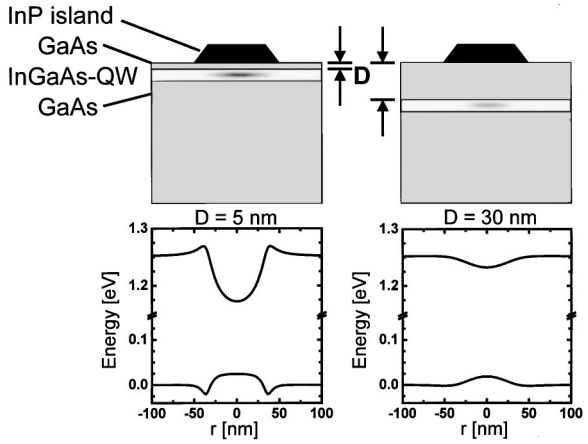


FIG. 1. Illustration of the sample design showing the effect of the thickness $D$ of the upper GaAs spacer layer on the conduction- and valence-band profiles of the buried InGaAs quantum well. When the thickness $D$ is small (left), the strain underneath the InP island has its strongest effect on the depth of the quantum dot potential, whereas a larger $D$ (right) reduces the depth of the quantum dot potential.

the QD potentials as sketched in the lower part of Fig. 1. Details about the sample growth and structure can be found elsewhere.[19–21] In this paper a set of four samples is analyzed, where the thickness $D$ of the top GaAs spacer layer is set to 5, 12, 20, and 30 nm. All experiments are carried out in a cryostat cooled by liquid helium to $T=25$ K. The samples are mounted on a single copper block using heat-conducting silver paste. This allows us to quantitatively compare the photoluminescence intensities of the four samples, since the cooled cryostat is moved by only a few millimeters in the lateral direction to take the spectrum of adjacent samples.

We perform time-integrated photoluminescence measurements by using a mode-locked Ti:sapphire laser with a repetition rate of 82 MHz and typical pulse widths of 80 fs as an excitation source. Nonresonant excitation of the QD's in the GaAs barrier or, alternatively, in the InGaAs QW, is carried out. In order to excite in the GaAs barrier material we use an excitation wavelength of 800 nm (i.e., 1.55 eV), and for excitation in the QW an excitation wavelength of 840 nm (i.e., 1.48 eV). With a typical spot size of about 150 $\mu$m, we estimate the number of QD's in the excited region to be $1.7\times10^5$. The collected luminescence is detected by a single-grating charge-coupled device spectrometer.

The time-resolved measurements are carried out by using the spectrometer as a monochromator and placing a Si-based avalanche photodiode behind the exit slit. Standard time-correlated single-photon counting is performed under excitation with the 80 fs pulses from the mode-locked Ti:sapphire laser. The time resolution of this setup is mainly determined by the time jitter of the avalanche photodiode and amounts to about 300 ps.

## III. RESULTS OF TIME-INTEGRATED MEASUREMENTS

Figure 2(a) shows a sketch of the energy level scheme of the QD's. They exhibit equally spaced energy levels, due to the almost parabolic in-plane confinement potential. In these QD's only transitions with identical main quantum number

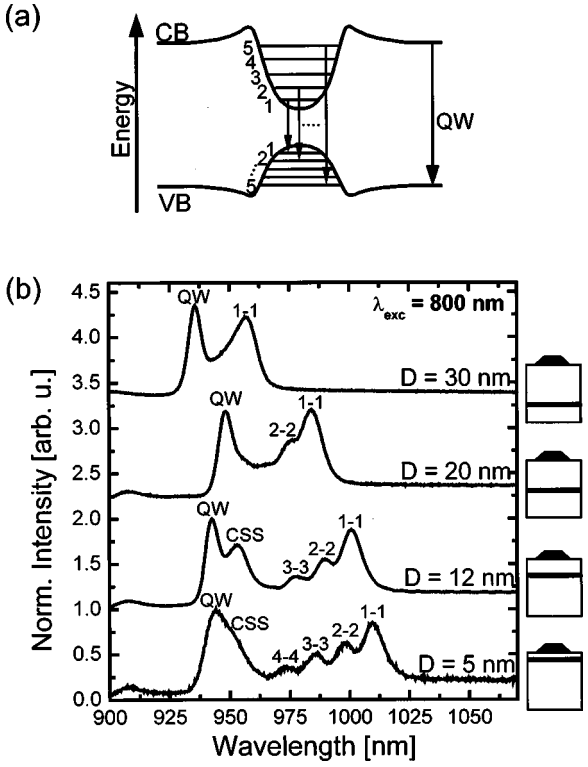


FIG. 2. (a) Schematic of the conduction band (CB) and valence band (VB) of the strain-induced quantum dots with energy levels and transitions. (b) Normalized photoluminescence spectra of all four samples with varying spacer layer thickness $D$ upon excitation in the GaAs barrier material at 800 nm. The thickness $D$ of the top GaAs spacer layer is written adjacent to the curves. The spectra are shifted by a constant value for clarity. The numbers 1-1, . . . ,4-4 denote the QD transitions, while QW and CSS denote the quantum well and charge-separated state transitions, respectively.

for electrons and holes are dipole allowed;[22] we therefore number the transitions as 1-1, 2-2, etc. Figure 2(b) shows the dependence of the transition energies on the spacer layer thickness $D$ in photoluminescence measurements upon nonresonant excitation in the GaAs barrier material at 800 nm. An energy density of 0.14 $\mu$J/cm$^2$ per pulse is used, which corresponds to an excitation density of $5.8\times10^{15}$ cm$^{-3}$. When the QW lies close to the surface ($D=5$ nm), the QD ground state (1-1) transition at 1010 nm as well as up to four transitions from excited states are detected. As $D$ is increased (i.e., the QW is moved further away from the surface), two observations are made. First, the QD ground state transition shifts toward higher energies. Secondly, the level spacing of the excited states within the QD decreases. These findings are a consequence of the decreasing depth of the QD potential (illustrated in Fig. 1); if $D$ is small, the strain underneath the InP islands results in a large modulation of the QW band gap. Moving the QW away from the stressors results in a smaller band-gap modulation.[21] In the spectrum for $D=30$ nm no separation between the energy levels is observed due to the spectral width of each transition of approximately 10 nm. Instead, only a broad shoulder on the high-energy side of the ground state transition indicates the presence of excited state transitions. For $D=5$, 12, 20 nm, there is an additional transition observable at the low-energy side of the QW transition. This transition is ascribed to the charge-

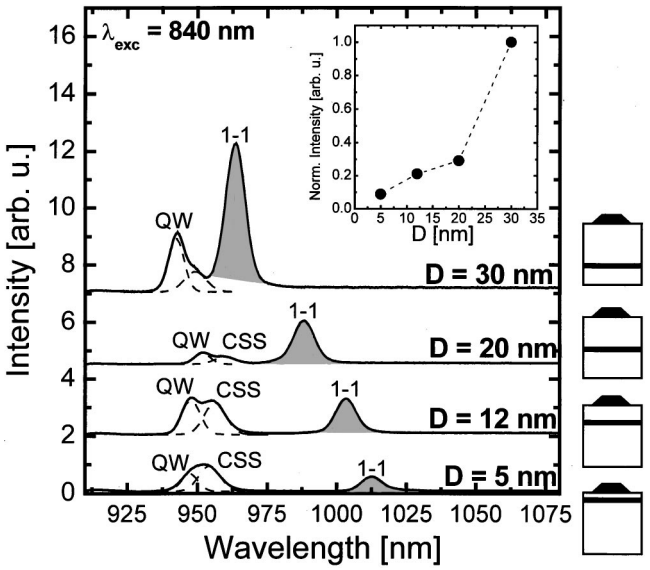


FIG. 3. Photoluminescence spectra upon nonresonant excitation in the InGaAs quantum well at 840 nm excitation wavelength for varying thickness $D$ of the GaAs spacer layer. The quantum dot ground state transitions (1-1) are shaded. The dashed lines are Gaussian fits to resolve the QW and CSS lines. The spectra are shifted by a constant value for clarity. The inset shows the intensity of the quantum dot ground state transition as a function of $D$.

separated state (CSS) suggested by Gu and co-workers,[23,24] which consists of an electron at the QW conduction-band edge bound to a hole in the QD ground state. This state is long lived since the in-plane potential barrier situated below the stressor-island edge (Fig. 1, top left), which is induced by compressive strain, slows down capture of the electron into the QD. Since there is some finite overlap between the electron and hole wave functions, the CSS appears as an optical transition in the photoluminescence spectra.

This paper focuses on the capture of QW carriers into the QD ground state as a function of the QW/surface separation $D$. To avoid the carrier dynamics in the GaAs obscuring the dynamics of interest, it is desirable not to excite in the GaAs, but in the QW. In Fig. 3 photoluminescence spectra for excitation in the InGaAs QW (excitation wavelength 840 nm) are shown for all four samples. The energy density per pulse is again 0.14 $\mu$J/cm$^2$, as in Fig. 2. However, since the excitation volume is much smaller than for excitation in the GaAs, we estimate that a factor of 45 fewer electron-hole pairs are excited in the QW.[25] This means that the estimated average number of electron-hole pairs per QD is much less than 1. Consequently, the time-integrated spectra in Fig. 3 show only the QD ground state transitions (gray shaded areas) and no higher QD transitions; the latter appear in the spectra only if the carrier occupation is large enough that Pauli blocking slows down the carrier relaxation. The spectra also show the QW and CSS transitions, which we separate from each other using a simple line fit (dashed lines). A crucial observation is that the *1-1 luminescence intensity increases considerably with increasing spacer layer thickness D*. This is also shown in the inset of Fig. 3, where the spectrally integrated luminescence intensity of the 1-1 transition is plotted versus $D$.

For the interpretation of the $D$-dependent spectra in Fig. 3, it is useful to consider the level scheme in Fig. 4(a), which shows the decay channels of the QW carriers. First, carriers in the QW can recombine radiatively (curved arrow) and nonradiatively [for example, via carrier tunneling into surface states (SS's)]. Alternatively, the QW carriers can be captured into the QD and relax into the QD ground state (for simplicity the internal level structure of the QD is not shown here). These QD carriers may recombine either radiatively or nonradiatively, e.g., via tunneling into surface states (similarly to the QW case). In an alternative process, the QW carriers may also get trapped into the CSS, from where they can decay radiatively or nonradiatively via capture of the electron into the QD. Due to the complicated nature of the level scheme in Fig. 4(a), we propose a simplified level scheme as shown in Fig. 4(b). Here, the CSS is neglected and carriers in the QW follow three different decay paths. These are radiative recombination with rate $\gamma_{R,\mathrm{QW}}$, nonradiative recombination with rate $\gamma_{\mathrm{NR,\,QW}}$, and capture into the QD ground state at a rate $\gamma_{\mathrm{cap}}$ (which includes both capture into the QD and subsequent relaxation to the ground state). From the QD ground state, QD carriers may decay either radiatively at rate $\gamma_{R,\mathrm{QD}}$ or nonradiatively at rate $\gamma_{\mathrm{NR,\,QD}}$. Our omission of the CSS in the simplified scheme can be understood as follows. As we will show in Sec. IV of this paper, the decay from the CSS into the QD is slow compared to direct capture from the QW into the QD. Therefore the CSS contributes little to the QD photoluminescence intensity in Fig. 3. As far as the $D$ dependence of the QD photoluminescence intensities in Fig. 3 is concerned, we may therefore neglect the CSS channel for the moment.

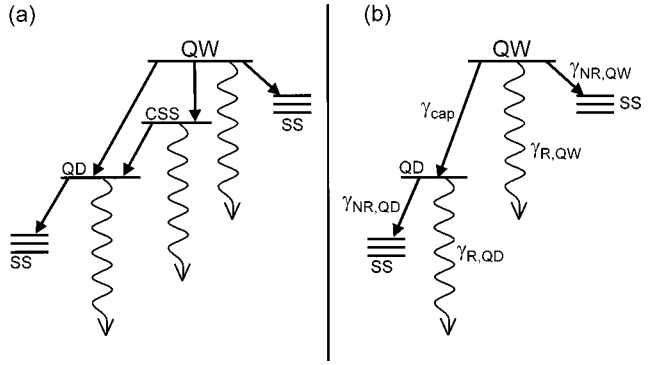


FIG. 4. Decay diagrams for quantum well carriers. The straight arrows are nonradiative decay paths, the curved lines represent radiative recombination. (a) Exact decay diagram. (b) Simplified decay diagram as explained in the text.

We now return to the $D$ dependence of the QD 1-1 luminescence intensity in Fig. 3. In the following, we attempt to trace back this $D$ dependence to possible $D$ dependencies of the various rates indicated in Fig. 4(b). These possible $D$ dependencies are listed below.

(a) The QW nonradiative recombination rate $\gamma_{\mathrm{NR,\,QW}}$ is expected to be strongly dependent on $D$, since carrier tunneling into surface states should become more efficient with decreasing QW/surface separation.

(b) The capture rate of QW carriers into the QD ground state $\gamma_{\mathrm{cap}}$ may vary with $D$ due to the $D$ dependence of the QD confinement potential.

(c) The QD radiative recombination rate $\gamma_{R,\mathrm{QD}}$ may depend on $D$, since the spatial extension of the electron and

hole wave functions should decrease with increasing QD confinement potential depth.[26,27]

(d) For the same reason as in (a), the QD nonradiative recombination rate $\gamma_{\mathrm{NR,QD}}$ may depend on $D$.

(e) In contrast to (c), it is safe to assume that the QW radiative recombination rate $\gamma_{R,\mathrm{QW}}$ is *independent* of $D$.

In the following, we will analyze which of the possible $D$ dependencies (a)–(d) contribute to the $D$ dependence of the QD 1-1 luminescence intensity. To this end, we consider the (time-dependent) total number of electron-hole pairs in the QW in the excitation region, $N_{\mathrm{QW}}(t)$. In the low-excitation limit, where Pauli blocking effects can be neglected, $N_{\mathrm{QW}}$ will decay according to

$$N_{\mathrm{QW}}(t)=N_{\mathrm{QW}}(0)\exp[-(\gamma_{\mathrm{cap}}+\gamma_{R,\mathrm{QW}}+\gamma_{\mathrm{NR,QW}})t]. \quad (1)$$

Simultaneously, the number of electron-hole pairs captured from the QW into the QD's will increase according to

$$\frac{dN_{\mathrm{cap}}}{dt}=\gamma_{\mathrm{cap}}N_{\mathrm{QW}}(t). \quad (2)$$

Inserting Eq. (1) into Eq. (2) and integrating over time yields the total number of electron-hole pairs captured into the QD's:

$$N_{\mathrm{cap}}=\frac{\gamma_{\mathrm{cap}}}{\gamma_{\mathrm{cap}}+\gamma_{R,\mathrm{QW}}+\gamma_{\mathrm{NR,QW}}}N_{\mathrm{QW}}(0). \quad (3)$$

An analogous relation is obtained for the total number of QW electron-hole pairs undergoing radiative recombination, $N_{R,\mathrm{QW}}$. Combining this relation with Eq. (3) yields

$$\frac{N_{\mathrm{cap}}}{N_{R,\mathrm{QW}}}=\frac{\gamma_{\mathrm{cap}}}{\gamma_{R,\mathrm{QW}}}. \quad (4)$$

This would allow us to determine the capture rate into the QD's, $\gamma_{\mathrm{cap}}$, if the other three quantities in Eq. (4) were known. The total number of electron-hole pairs captured into the QD's ($N_{\mathrm{cap}}$) and the total number of QD carriers recombining radiatively ($N_{R,\mathrm{QD}}$) are related via

$$N_{R,\mathrm{QD}}=\eta_{\mathrm{QD}}N_{\mathrm{cap}}, \quad (5)$$

where $\eta_{\mathrm{QD}}$ is the QD quantum efficiency. Inserting Eq. (5) into Eq. (4) yields

$$\gamma_{\mathrm{cap}}\eta_{\mathrm{QD}}=\frac{N_{R,\mathrm{QD}}}{N_{R,\mathrm{QW}}}\gamma_{R,\mathrm{QW}}. \quad (6)$$

Expressing the ratio of carrier numbers $N_{R,\mathrm{QD}}/N_{R,\mathrm{QW}}$ by the ratio of the respective photoluminescence intensities $I_{R,\mathrm{QD}}/I_{R,\mathrm{QW}}$, and expressing the rates in terms of the respective time constants, one finally obtains

$$\tau_{\mathrm{cap}}/\eta_{\mathrm{QD}}=\frac{I_{R,\mathrm{QW}}}{I_{R,\mathrm{QD}}}\tau_{R,\mathrm{QW}}. \quad (7)$$

Equation (7) implies that the quantity $\tau_{\mathrm{cap}}/\eta_{\mathrm{QD}}$ can be determined from the ratio of the QW and QD photoluminescence intensities in Fig. 3, provided that $\tau_{R,\mathrm{QW}}$ is known. $\tau_{R,\mathrm{QW}}$ obviously cannot be determined directly from time-resolved measurements on the present structures, due to the presence of the nonradiative processes. We resort to adopting an exciton lifetime of $\tau_{R,\mathrm{QW}}=300$ ps as determined by a time-resolved photoluminescence measurement on a similar near-surface InGaAs QW structure that contained no stressor islands, but was covered with a thin InP surface passivation layer to reduce surface recombination.[28] For comparison we note that similar values of around 500 ps for the radiative lifetime in deep InGaAs QW's have been reported in the literature.[29,30]

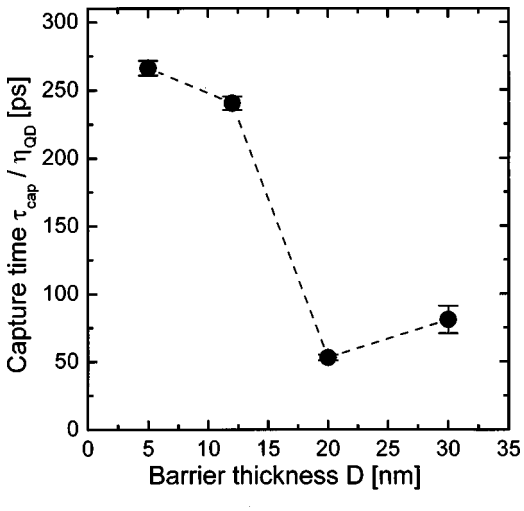


FIG. 5. Calculated quantum dot capture time $\tau_{\mathrm{cap}}/\eta_{\mathrm{QD}}$ versus the GaAs spacer thickness $D$ according to Eq. (7). The error bars reflect the uncertainties in $I_{\mathrm{R,QD}}$ and $I_{\mathrm{R,QW}}$, as described in the text.

Figure 5 shows the quantity $\tau_{\mathrm{cap}}/\eta_{\mathrm{QD}}$ determined from Eq. (7) for all GaAs spacer thicknesses $D$. The errors bars originate from the uncertainties in $I_{R,\mathrm{QW}}$ and $I_{R,\mathrm{QD}}$, which are taken from the fits to the peaks in Fig. 3. The general trend is clearly visible: as the QW is moved further away from the surface, $\tau_{\mathrm{cap}}/\eta_{\mathrm{QD}}$ decreases from 260 ps for the $D=5$ nm sample to around 80 ps for the $D=30$ nm sample. If the QD quantum efficiency $\eta_{\mathrm{QD}}$ was 100% for all $D$, Fig. 5 would directly give the dependence of the capture time on $D$, and thus on the confinement potential, as described in point (b) of the above list. However, if $\eta_{\mathrm{QD}}<100\%$, the $D$ dependence of $\tau_{\mathrm{cap}}/\eta_{\mathrm{QD}}$ could be caused by a possible $D$ dependence of $\eta_{\mathrm{QD}}$ and thus of the QD radiative/nonradiative recombination rates [points (c) and (d)]. In the following two sections, we will show that $\eta_{\mathrm{QD}}$ is in fact independent of $D$, and that, consequently, all $D$ dependence of $\tau_{\mathrm{cap}}/\eta_{\mathrm{QD}}$ in Fig. 5 is caused by that of $\tau_{\mathrm{cap}}$.

## IV. RESULTS OF TIME-RESOLVED MEASUREMENTS

In the following, we will present the results of time-resolved measurements of the decay time of the QD 1-1 transition, $\tau_{\mathrm{dec,QD}}$. This will help us to determine $\eta_{\mathrm{QD}}$ since

$$\eta_{\mathrm{QD}}=\frac{\tau_{R,\mathrm{QD}}^{-1}}{\tau_{R,\mathrm{QD}}^{-1}+\tau_{\mathrm{NR,QD}}^{-1}}=\frac{\tau_{R,\mathrm{QD}}^{-1}}{\tau_{\mathrm{dec,QD}}^{-1}} \quad (8)$$

The results from time-resolved photoluminescence measurements of the QD 1-1 decay are shown in Fig. 6. The excitation conditions in the time-integrated (Fig. 3) and time-resolved (Fig. 6) measurements are identical, which is essential for comparison of the data. All transients show an initial signal rise that is not time resolved with this tech-

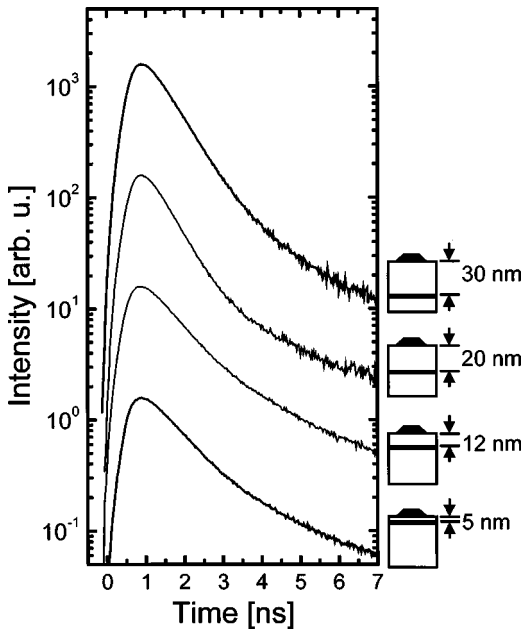


FIG. 6. Quantum dot ground state decay curves upon nonresonant excitation in the InGaAs quantum well at 840 nm excitation wavelength for varying GaAs spacer thickness *D*. The curves are shifted by a constant factor for clarity.

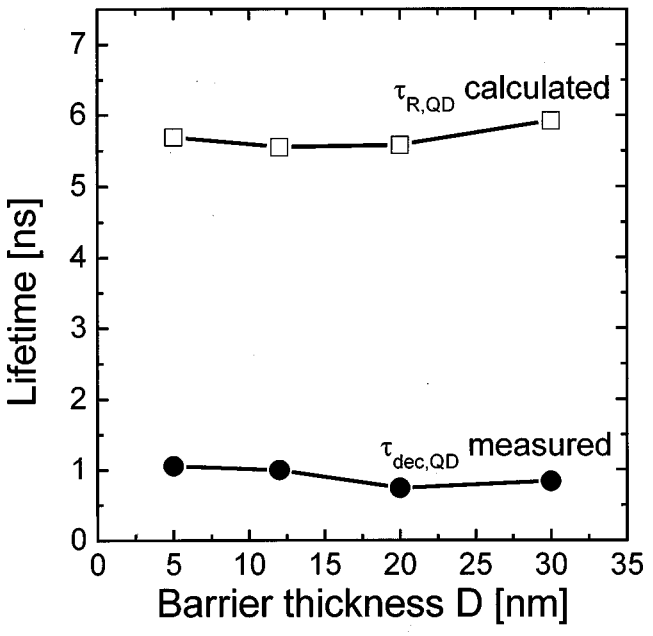


FIG. 7. Measured quantum dot ground state decay time $\tau_{\mathrm{dec,QD}}$ from Fig. 6 (fast-decay component) and calculated radiative decay time $\tau_{R,\mathrm{QD}}$ as a function of the thickness *D* of the top GaAs spacer layer.

nique. The decay of all four curves is biexponential, with time constants of ≈1 and ≈4 ns, respectively. A similar two-component decay has been observed in Ref. 24; the fast component was assigned to carriers that are captured directly into the QD. This initial decay yields the lifetime of the QD ground state transition. The slow component was identified as a consequence of the charge-separated state.[24] This long-lived state acts as a reservoir and slowly feeds electrons into the QD ground state. Numerically integrating both photoluminescence components separately over time yields their respective contributions to the QD 1-1 photoluminescence intensity in the spectra of Fig. 3. It turns out that for all *D* this contribution never exceeds 30% of the QD 1-1 photoluminescence intensity, which justifies our omission of the CSS channel in the simplified level scheme of Fig. 4(b). However, in our quantitative evaluation of Eq. (7) leading to Fig. 5, we have taken this component into account by subtracting it from the QD 1-1 photoluminescence intensity in Fig. 3 before calculating $\tau_{\mathrm{cap}}/\eta_{\mathrm{QD}}$.

In Fig. 7 the time constant of the fast decay $\tau_{\mathrm{dec,QD}}$ (solid circles) is plotted versus the spacer layer thickness *D*. While the decay times of the 5 and 12 nm samples are slightly longer (≈1.0 ns) than for the 20 and 30 nm samples (≈0.8 ns), no significant trend is observed. We may therefore conclude that $\tau_{\mathrm{dec,QD}}$ is essentially independent of *D*. To determine the QD quantum efficiency $\eta_{\mathrm{QD}}$ according to Eq. (8), it now remains to be determined what *D* dependence (if any) the QD radiative recombination lifetime $\tau_{R,\mathrm{QD}}$ has. To this end, $\tau_{R,\mathrm{QD}}$ will be calculated theoretically in the following section.

## V. CALCULATIONS

The calculation of the radiative recombination lifetime $\tau_{R,\mathrm{QD}}$ of the QD ground state transition is performed in three steps. In a first step, the strain-induced modulation of the QW valence and conduction bands is calculated. This is done by using a finite element method, which is described in detail in Ref. 22. In this reference, plots of a typical calculated QD potential are shown as a function of the depth *z* from the surface and radial distance *r* from the center of the InP island. In a second step, the electron and hole wave functions for the QD ground state are calculated as functions of *r* and *z*.[22] For this purpose the standard Luttinger-Kohn Hamiltonian[31] is added to a strain Hamiltonian that takes into account the strain interaction for the conduction and valence bands.[32,33] The angular part of the wave function $\psi$ can be separated,

$$\psi(r,z,\phi)=F(r,z)e^{-im\phi}, \tag{9}$$

where *m* is the angular momentum quantum number; $m=0$ for the ground state transition.

Finally, the electron and hole wave functions are factored as $F(r,z)=F(r)g(z)$ (an approximation that we have verified holds to very high accuracy), and the electron-hole pair wave functions $F_{eh}(r_e,r_h,z_e,z_h)$ are constructed as products of electron and hole wave functions. These can be well approximated by

$$F_{eh}(r_e,r_h,z_e,z_h)=f_{eh}(R)h_{eh}(\rho)g_e(z_e)g_h(z_h),$$

where *R* is the electron-hole in-plane center-of-mass coordinate and $\rho$ is the in-plane relative coordinate. We thus obtain an electron-hole wave function whose form is analogous to an exciton in a quantum well whose center-of-mass motion is localized by well-width fluctuations. To calculate the radiative lifetime, we apply the model of Refs. 27 and 34, assuming that spin relaxation is fast as compared to the radiative decay. Figure 7 shows the calculated radiative lifetimes $\tau_{R,\mathrm{QD}}$ as a function of the thickness *D* (open squares). They

are essentially independent of $D$. This is mainly due to the fact that the spatial widths of the calculated ground state wave functions only vary by 10–15 % when $D$ is increased from 5 to 30 nm. $\tau_{R,\mathrm{QD}}$ lies at remarkably high values between 5.5 and 6 ns. In order to interpret these high values it has to be noted that not only the overlap of the electron and hole wave functions enters into these calculations (according to Fermi's golden rule). In addition, the spatial extent of the center-of-mass part of the wave function determines the efficiency of the coupling to the light.[26] In recent calculations this effect was not taken into account.[14] In this reference an independent-particle model was used, assuming complete screening of the particle-particle Coulomb interaction, and a much smaller value of $\tau_{R,\mathrm{QD}}=0.7$ ns was calculated.

The discrepancy between the radiative lifetime $\tau_{R,\mathrm{QD}}$ calculated here and the measured lifetime $\tau_{\mathrm{dec,QD}}$ implies a quantum efficiency $\eta_{\mathrm{QD}}$ of only 15–20 % according to Eq. (8). This low quantum efficiency is essentially independent of the QW/surface separation $D$. This independence of $D$ precludes carrier tunneling into surface states as the dominant mechanism for the nonradiative recombination of QD carriers. Alternative mechanisms could involve intrinsic nonradiative decay channels within the QD's, which, however, are unlikely given the high quality of the strain-induced QD structures. It is also possible that our theoretical assumption of fast spin relaxation must be called into question for the QD's.[35] A slower spin relaxation would lead to shorter radiative lifetimes $\tau_{R,\mathrm{QD}}$ for all $D$, and thus to a better agreement with the measured decay times.

## VI. DISCUSSION

Whatever the reason for the discrepancy between the calculated radiative lifetime $\tau_{R,\mathrm{QD}}$ and the measured lifetime $\tau_{\mathrm{dec,QD}}$, the important point in Fig. 7 is the absence of any significant dependence of the QD quantum efficiency on the QW/surface separation $D$. This result means that the strong $D$ dependence of $\tau_{\mathrm{cap}}/\eta_{\mathrm{QD}}$ in Fig. 5 is entirely due to the $D$ dependence of the capture time $\tau_{\mathrm{cap}}$. This is an important result it means that *the capture time depends on the strain-induced in-plane QD confinement potential*. In principle, there may be two main reasons why this should be so: With decreasing $D$, the confinement potential becomes *deeper* and the in-plane potential barriers situated below the stressor island edges become *higher*. A deeper confinement potential means that the QD states lie at lower energies and have wider energy separations, which is expected to slow down the capture into the QD's; this should be true for both phonon- and Coulomb-mediated capture processes. Higher in-plane potential barriers mean that QW carriers that are energetically at the bottoms of the QW subbands will find it increasingly difficult to tunnel into the QD's or become thermally activated across them. According to the theoretical calculation presented in Sec. V, the height of these potential barriers increases from 0.3 meV ($D=30$ nm sample) to 16.7 meV ($D=5$ nm sample) for the conduction band and from 2.1 meV ($D=30$ nm sample) to 20 meV ($D=5$ nm sample) for the valence band. However, the time constant of the slow-decay component in Fig. 6 (which is associated with the capture of electrons from the CSS into the QD's) shows very little dependence on the in-plane barrier height. We therefore conclude that *not the in-plane barrier height but the confinement potential depth is the decisive factor controlling* $\tau_{\mathrm{cap}}$.

So far we have verified point (b) and rejected points (c) and (d) in the list in Sec. III, using the photoluminescence-intensity ratios of the QW and QD 1-1 transitions as well as the results of time-resolved measurements and theoretical calculations. As yet it is not clear how far point (a) applies. Some conclusions about this point can be drawn from the photoluminescence intensity of the QW transition in the spectra of Fig. 3. This intensity decreases as $D$ is decreased from $D=30$ to 5 nm (with the exception of $D=20$ nm). This means that an increasing number of QW carriers undergoes nonradiative recombination. In other words, $\gamma_{\mathrm{NR,\,QW}}$ increases with decreased $D$ (again, $D=20$ nm is an exception, for reasons as yet unknown). This tendency is explained by the increased tunneling of carriers into surface states when the QW approaches the surface, and thus supports the statement made in point (a). In this context, it is remarkable that the same tendency does not apply to the nonradiative recombination of QD carriers; $\tau_{\mathrm{NR,\,QD}}$ has in fact been found, in the previous sections, to be independent of $D$. This may be due to the protective influence of the InP islands atop each QD, which form a tunneling barrier for the QD carriers.

## VII. CONCLUSION

In conclusion, we have investigated carrier capture processes in strain-induced quantum dot structures. A series of four samples with varying distance $D$ of the quantum well to the surface has been studied. Using time-integrated and time-resolved photoluminescence spectroscopy, we have shown that the carrier capture from the quantum well into the quantum dots accelerates considerably when the energetic depth of the confinement potential is reduced by enlarging $D$. Carriers in the quantum well region between the quantum dots have been found to experience nonradiative surface recombination, which accelerates with decreasing $D$. In contrast, no $D$ dependence of the nonradiative recombination rate has been found for carriers confined in the quantum dots. This indicates that surface recombination is negligible for quantum dot carriers, presumably due to the protecting InP islands.

## ACKNOWLEDGMENTS

The authors thank W. Stadler for technical help. We also thank R. T. Phillips and L. M. Herz for fruitful discussions. This work was supported by the Deutsche Forschungsgemeinschaft via Sonderforschungsbereich 348 and by the European Union via the TMR Network ''Ultrafast Quantum Optoelectronics.'' The work of M.W.F. and D.S.C. was funded by the Office of Naval Research and by the National Science Foundation under Grant No. DMR-9705403.

*Present address: INFINEON Technologies, Balanstraße 73, D-81541 München, Germany.

†Present address: Biomolecular Optics Group, Ludwig-Maximilians-Universität, Oettingenstraße 67, D-80538 Müchen,

Germany.
[1] M. Asada, Y. Miyamoto, and Y. Suematsu, IEEE J. Quantum Electron. **QE-22**, 1915 (1986).
[2] N. Kirstaedter, O. G. Schmidt, N. N. Ledentsov, D. Bimberg, V. M. Ustinov, A. Y. Egorov, A. E. Zhukov, M. V. Maximov, P. S. Kop'ev, and Z. I. Alferov, Appl. Phys. Lett. **69**, 1226 (1996).
[3] L. Harris, A. D. Ashmore, D. J. Mowbray, M. S. Skolnick, M. Hopkinson, G. Hill, and J. Clark, Appl. Phys. Lett. **75**, 3512 (1999).
[4] R. J. Warburton, B. T. Miller, C. S. Dürr, C. Bödefeld, K. Karrai, J. P. Kotthaus, G. Medeiros-Ribeiro, P. M. Petroff, and S. Huant, Phys. Rev. B **58**, 16 221 (1998).
[5] M. C. Bödefeld, R. J. Warburton, K. Karrai, J. P. Kotthaus, G. Medeiros-Ribeiro, and P. M. Petroff, Appl. Phys. Lett. **74**, 1839 (1999).
[6] U. Bockelmann and G. Bastard, Phys. Rev. B **42**, 8947 (1990).
[7] H. Benisty, C. M. Sotomayor-Torrés, and C. Weisbuch, Phys. Rev. B **44**, 10 945 (1991).
[8] M. Sugawara, K. Mukhai, and H. Shoji, Appl. Phys. Lett. **71**, 2791 (1997).
[9] Y. Zhang, M. D. Sturge, K. Kash, B. P. van der Gaag, A. S. Gozdz, L. T. Florez, and J. P. Harbison, Phys. Rev. B **51**, 13 303 (1995).
[10] J. H. H. Sandmann, S. Grosse, G. von Plessen, J. Feldmann, G. Hayes, R. Phillips, H. Lipsanen, M. Sopanen, and J. Ahopelto, Phys. Status Solidi A **164**, 421 (1997).
[11] J. H. H. Sandmann, S. Grosse, G. von Plessen, J. Feldmann, G. Hayes, R. Phillips, H. Lipsanen, M. Sopanen, and J. Ahopelto, Phys. Status Solidi B **204**, 251 (1997).
[12] S. Grosse, J. Sandmann, G. v. Plessen, J. Feldmann, H. Lipsanen, M. Sopanen, J. Tulkki, and J. Ahapelto, Phys. Rev. B **55**, 4473 (1997).
[13] M. Braskén, M. Lindberg, and J. Tulkki, Phys. Status Solidi A **164**, 427 (1997).
[14] M. Braskén, M. Lindberg, M. Sopanen, H. Lipsanen, and J. Tulkki, Phys. Rev. B **58**, 15 993 (1998).
[15] R. Rinaldi, P. V. Giugno, R. Cingolani, H. Lipsanen, M. Sopanen, J. Tulkki, and J. Ahopelto, Phys. Rev. Lett. **77**, 342 (1996).
[16] R. Rinaldi, R. Mangino, R. Cingolani, H. Lipsanen, M. Sopanen, J. Tulkki, M. Braskén, and J. Ahopelto, Phys. Rev. B **57**, 9763 (1998).
[17] R. Cingolani, R. Rinaldi, H. Lipsanen, M. Sopanen, R. Virkkala, K. Maijala, J. Tulkki, J. Ahopelto, K. Uchida, N. Miura, and Y. Arakawa, Phys. Rev. Lett. **83**, 4832 (1999).
[18] T. Lundstrom, W. Schoenfeld, H. L. Lee, and P. M. Petroff, Science **286**, 2312 (1999).
[19] M. Sopanen, H. Lipsanen, and J. Ahopelto, Appl. Phys. Lett. **66**, 2364 (1995).
[20] H. Lipsanen, M. Sopanen, and J. Ahopelto, Phys. Rev. B **51**, 13 868 (1995).
[21] J. Ahopelto, M. Sopanen, and H. Lipsanen, Jpn. J. Appl. Phys., Part 1 **38**, 1081 (1999).
[22] J. Tulkki and A. Heinämäki, Phys. Rev. B **52**, 8239 (1995).
[23] Y. Gu, M. D. Sturge, K. Kash, B. P. van der Gaag, A. S. Goszdz, L. T. Florez, and J. P. Harbison, Superlattices Microstruct. **19**, 131 (1996).
[24] Y. Gu, M. D. Sturge, K. Kash, N. Watkins, B. P. van der Gaag, A. S. Gozdz, L. T. Florez, and J. P. Harbison, Appl. Phys. Lett. **70**, 1733 (1997).
[25] We assume the same absorption in the quantum well for all four samples.
[26] E. I. Rashba and G. E. Gurgenishvili, Fiz. Tverd. Tela (Leningrad) **4**, 1029 (1962) [Sov. Phys. Solid State **4**, 759 (1962)].
[27] D. S. Citrin, Superlattices Microstruct. **13**, 303 (1993).
[28] H. Lipsanen, M. Sopanen, J. Ahopelto, J. Sandmann, and J. Feldmann, Jpn. J. Appl. Phys., Part 1 **38**, 1133 (1999).
[29] C. Rocke, A. O. Govorov, A. Wixforth, G. Böhm, and G. Weimann, Phys. Rev. B **57**, R6850 (1998).
[30] A. Wixforth, Physica E (Amsterdam) **3**, 145 (1998).
[31] T. B. Bahder, Phys. Rev. B **41**, 11 992 (1990).
[32] G. E. Pikus and G. L. Bir, Fiz. Tverd. Tela (Leningrad) **1**, 154 (1959) [Sov. Phys. Solid State **1**, 136 (1959)].
[33] D. Gershoni, C. H. Henry, and G. A. Baraff, IEEE J. Quantum Electron. **29**, 2433 (1993).
[34] D. S. Citrin, Phys. Rev. B **47**, 3832 (1993).
[35] J. A. Gupta, D. D. Awschalom, X. Peng, and A. P. Alivisatos, Phys. Rev. B **59**, R10 421 (1999).